OPEN ACCESS

Japanese Journal of Applied Physics **63**, 111007 (2024)

REGULAR PAPER

https://doi.org/**10.35848/1347-4065/ad8b8b**

Enhancement of removing OH bonds from low-temperature-deposited silicon oxide films by adding water vapor into NH_3 gas annealing at 130 °C

Susumu Horita*

School of Materials Science, Japan Advanced Institute of Science and Technology, Nomi, Ishikawa 923—1292, Japan

*E-mail: horita@jaist.ac.jp

Received October 9, 2024; revised October 23, 2024; accepted October 25, 2024; published online December 10, 2024

In this study, it is revealed that annealing with water-vapor-added NH_3 gas (water-added NH_3) is more effective than with dry NH_3 at removing residual OH bonds in silicon oxide (SiOx) films deposited by atmospheric chemical vapor deposition with an organic silicon source. Fourier transform infrared spectra showed that the reduction amount of OH bonds using the water-added NH_3 was ~4 or ~1.3 times larger than using the conventional dry N_2 or dry NH_3 mixed with N_2 gas without water, respectively. This result is somewhat surprising because water is a potential candidate as a source of OH. The effect of water vapor on OH bond removal can be explained by considering the following three factors; the first is that low-temperature SiOx films are constrained somewhat, the second is that strained Si-O-Si bonds are in a higher or more unstable energy state than strain-free ones, and the third is that highly strained bonds are easily hydroxylated to form Si-OH bonds.

1. Introduction

Low-temperature silicon oxide (SiOx) films are desired for the fabrication of not only thin-film transistors on non-heat-resistant substrates[1] but also interlayer dielectrics in order to avoid disconnection of the interconnect metal, redistribution of the dopant, and defect generation in the fabricated underlay with the advances in miniaturization of integration processes.[2] However, lower-temperature Si oxide films prepared by CVD methods with organic silicon sources such as tetraethylorthosilicate [TEOS: $Si(OC_2H_5)_4$] are more likely to contain a larger amount of OH bonds.[3–6] It is well known that OH bonds lead to serious problems of high leakage current and low breakdown voltage.[7–9] Therefore, after the film deposition, higher-temperature annealing is required, generally at above 350 °C, to remove them sufficiently,[10] which may not offer a true low-temperature process.

To overcome this difficulty, we have reported the use of ammonia (NH_3) as an atmosphere gas for annealing to remove the residual OH content, instead of the nitrogen (N_2) commonly used. Fourier transform infrared (FT-IR) spectra of the annealed films showed that the height of peaks due to OH bonds was reduced more than 1.5 times with NH_3 compared with only N_2 gas. This effect can be explained by the catalytic action of NH_3 as a Lewis base.[11] Recently, we found that adding water vapor into NH_3 gas enhances the removal of residual OH bonds in SiOx films.[12] This result seems somewhat surprising as water is a potential candidate as the source of OH bonds.

In this paper, we present not only the enhancement effect on the removal of OH bonds in SiOx films by adding water vapor into NH_3 gas, but also the film structure, which was different from that annealed with dry NH_3 gas, showing the experimental results of the FT-IR spectra. Finally, we discuss the mechanism of the removal of OH bonds by using the water vapor, correlating with the structural change in the SiOx films due to the annealing.

2. Experimental methods

Si oxide films were deposited on n-type (111)-oriented Si substrates by atmospheric pressure chemical vapor deposition. The details are mentioned elsewhere.[13,14] Prior to the deposition of the Si oxide films, the Si substrates were cleaned by a standard chemical-cleaning method which is so called RCA, and dipped into diluted hydrogen fluoride (HF) solution to remove the chemical oxide from the substrates. As a deposition source for Si oxide film, silicone oil (SO) of decamethylcyclopenta-siloxane ($C_{10}H_{30}O_5Si_5$) was used with ozone (O_3) gas at a concentration of ~150 g m^{-3}. The O_3 was generated using a silent electric discharge from 99.9995% O_2 gas at a flow rate of 0.50 lm (liters per minute at 25 °C). The SO was heated to around 50 °C and vaporized by bubbling with N_2 at a flow rate of 0.21 to 0.26 lm. To enhance the deposition rate, we also added trichloroethylene (C_2HCl_3: TCE), which was bubbled with N_2 gas at a flow rate of 0.1 lm, and the vapor was introduced into the chamber together with SO and O_3. The films were deposited for 10 min at 190 °C, and the film thickness was 80 to 90 nm. The surface of the as-deposited SiOx films is very unstable and chemically reactive since the low-temperature process is not in thermal equilibrium. Therefore, immediately after removing the deposited samples from the deposition chamber, they were immersed in ethanol solution to prevent a chemical reaction with atmospheric impurities such as water or oxygen.

Figure 1 shows a schematic diagram of the annealing apparatus to remove OH bonds in the SiOx films. Annealing was performed under the following three atmospheric gases: (1) N_2 (99.995%) gas at a flow rate of 0.4 lm, (2) 0.2-lm-NH_3 (99.999%) gas + 0.2-lm-N_2 gas (dry NH_3 gas, or "Dry"), and (3) $NH_3 + N_2$ gas with the addition of room temperature (RT) water vapor (water-added NH_3 gas, or "Water-added"). The water vapor was produced by bubbling RT H_2O solution with 0.4-lm-N_2 or 0.2-lm-NH_3 + 0.2-lm-N_2 by changing the flow direction of the annealing gas through a three-way valve as

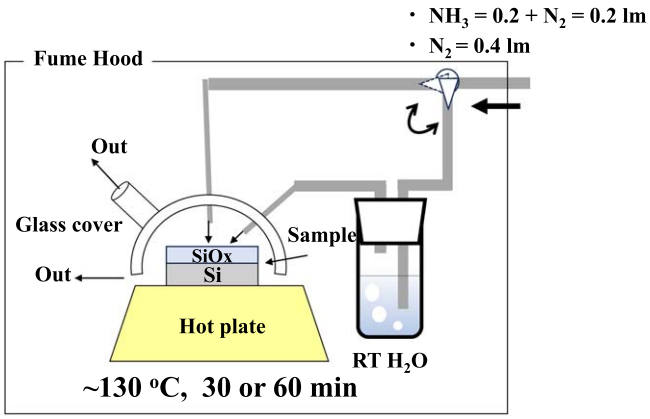

Fig. 1. Schematic diagram of the annealing apparatus used in this study to remove OH bonds in Si oxide films. The apparatus was placed in a fume hood to exhaust the used gases. The annealing gases were (1) N_2 (99.995%) gas at a flow rate of 0.4 lm at 25 °C, (2) NH_3 (99.999%) gas at 0.2 lm + N_2 gas at 0.2 lm, and (3) the (2) gas with the addition of RT water vapor. The water vapor was produced by bubbling H_2O with the annealing gas, whose flow direction was changed by a three-way valve. The samples set on the hot plate were annealed at 130 °C for a total time of 30 or 60 min.

shown in Fig. 1. In this case, the water vapor pressure was roughly estimated to be $\sim 3 \times 10^3$ Pa at RT. The sizes of the pipe and glass reactor and so on in Fig. 1 are reported elsewhere.[11] The annealing temperature and total time were 130 °C, and 30 or 60 min, respectively. After annealing, the samples were immersed in ethanol solution quickly in the same way as after deposition.

The thickness d was measured by ellipsometry with a 632.8 nm He–Ne laser beam. The molecular structures of the films were analyzed from the FT-IR spectra with a resolution of 4 cm^{-1} and the acquired spectra were averaged from ten scans. The measured FT-IR spectra were normalized by the highest peak of the Si-O-Si unsymmetric stretching (TO_3) vibration mode at around 1065 cm^{-1} as shown in Fig. 2(a) later.[15–17] In addition, the normalized spectra were smoothed by two runs of five points in order to improve the signal-to-noise ratio, and the first derivate of the averaged spectra was taken to estimate the width of the TO_3 mode peak instead of the full width at half maximum.[18] The details of the algorithms and derivation have been reported previously.[19] For a quantitative amount of OH content in deposited SiOx films, we used a characteristic value of S_{OH2} in the FT-IR spectra. The S_{OH2} is an integrated area of normalized absorbance intensity from 3050 to 3700 cm^{-1} of a broad peak due to O-H vibrations of Si-OH bonds and H_2O as shown in Fig. 3(b) later.[15,17,20] In this paper, this broad peak is labeled as OH2 following our previous paper, and also the peak at around 940 cm^{-1} due to Si-OH vibration is labeled as OH1.[19]

3. Results

Figure 2(a) shows the FT-IR spectra of SiOx films annealed in N_2 gas, dry NH_3 gas, and water-added NH_3 gas, compared with an as-deposited film as a reference. In each spectrum, the peaks at ~800 and 1070 cm^{-1} are identified as absorptions due to the bending (TO_2) and asymmetric stretching (TO_3) modes, respectively, of the Si-O-Si bond.[21–24] From this, it can be seen that the chemical composition of all the deposited SiOx films is roughly similar to that of thermal Si oxide films except for the peaks due to Si-OH vibration at

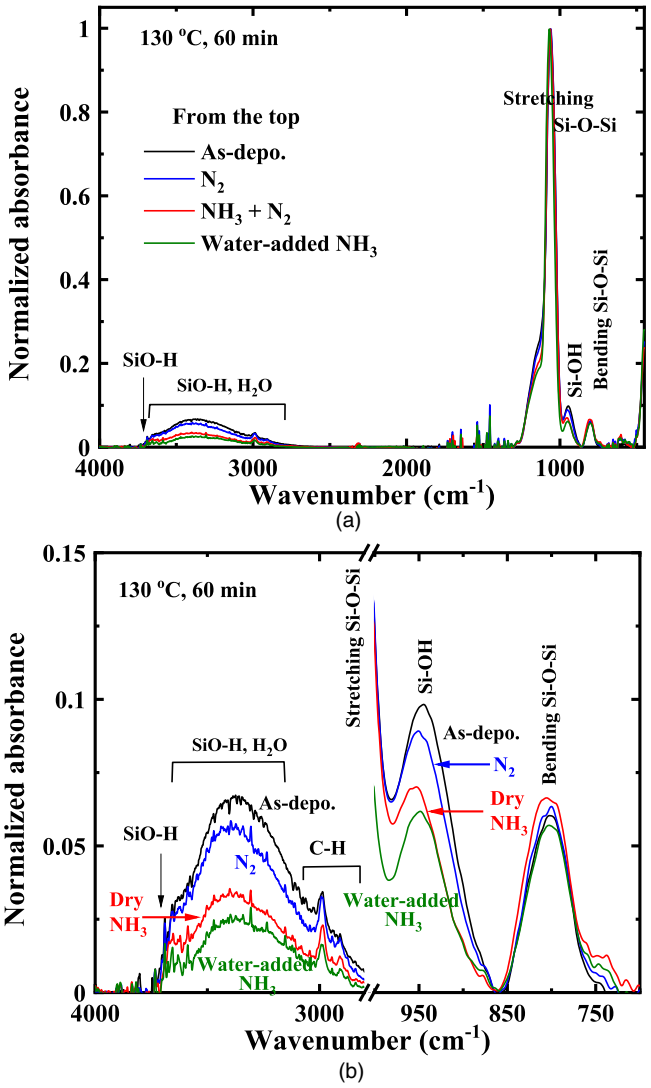

Fig. 2. FT-IR spectra of the Si oxide films annealed in N_2 gas, $NH_3 + N_2$ gas, and water-added NH_3 gas, compared with an as-deposited film as a reference, where their intensities are normalized with the highest peak of the asymmetric stretching (TO_3) mode of the Si-O-Si bond. (a) shows the wide-range spectra to view the whole, and (b) shows the two narrow-range spectra from 700 to 1030 and 2800 to 4000 cm^{-1} so as to easily observe the difference in peak intensity.

around 960 cm^{-1} and the broad peaks due to SiO-H and/or H-OH vibration at around 3400 cm^{-1}. These OH-related peaks are very often observed in Si oxide films deposited by common low-temperature deposition methods using organic silicon deposition sources without any post-treatment.[3–5,7,8,25] Figure 2(b) shows the expanded spectra of Fig. 2(a) in order to clearly see the difference in intensity among the three types of annealing gas. From all cases of annealing gas, it can be seen that both the ~950 and 3000 to 3700 cm^{-1} peaks are reduced even at a low temperature of 130 °C. Particularly, for the two cases with NH_3 gas, the reduction of OH bonds is much greater than that with only N_2 gas. This effective reduction is due to the catalytic action of NH_3 as a Lewis base to acidic Si-OH species through the dehydroxylation reaction

$$\mathrm{Si-OH + Si-OH \rightarrow Si-O-Si + H_2O\uparrow}, \qquad (1)$$

as mentioned previously.[11] Furthermore, it is noticeable that the water-added NH_3 gas removes a greater amount of OH

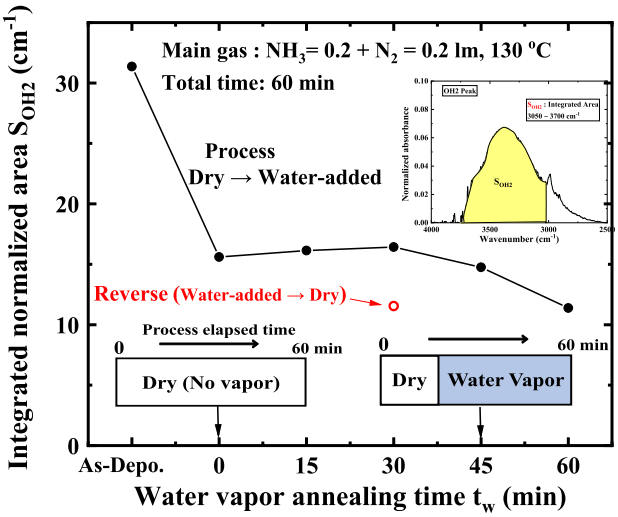

Fig. 3. Dependence of the integrated area 3050 to 4000 cm^{-1}, S_{OH2}, due to OH-related bonds as shown in the inset on the water vapor annealing time t_w after dry NH_3 annealing. The total annealing time is 60 min. $t_w = 0$ and 60 min indicate the 60-min dry NH_3 annealing without water vapor and the 60-min water-added NH_3 annealing, respectively. The black closed circles indicate the data for the dry → water-added NH_3 gas process, and the red open circle for the reverse process of the water-added → dry NH_3 gas.

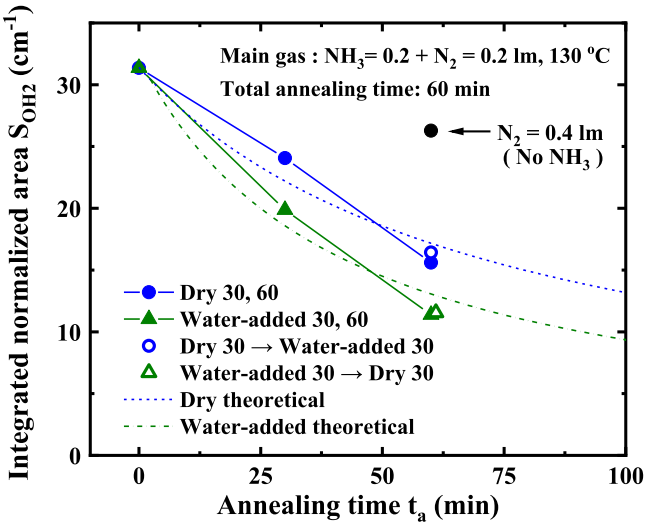

Fig. 4. Relationship between S_{OH2} and the total annealing time t_a for the dry (blue closed circles) and water-added (green closed triangles) NH_3 gas processes, in addition to the three results of the 30 min dry → 30 min water-added (blue open circle) process, vice versa (green open triangle), and only N_2 gas (no NH_3) annealing process (black closed circle) for comparison. The blue broken and the green dotted broken lines indicate theoretical calculation curves for the dry and the water-added cases, respectively, without changing the process gas, which is mentioned in detail in Sect. 4.

bonds than the dry NH_3 gas without water vapor. This is a surprising result as it can be considered simply that the water-added gas should increase the amount of residual OH bonds in the SiOx films since H_2O is one of the sources of OH bonds. On the other hand, we notice C-H-related peaks at around 3000 cm^{-1}. These peaks are a result of the alkoxylation reaction owing to immersing the samples in ethanol[26–28] because such C-H peaks in an as-deposited film are never observed without immersing in ethanol.

In order to further investigate the water vapor effect in annealing on the reduction of OH bonds in the SiOx films, we tried to change the annealing gaseous species in the middle of annealing, i.e. from dry NH_3 to water-added NH_3 gas and vice versa, keeping the total annealing time of 60 min. The closed black circles in Fig. 3 show the dependence of the integrated area due to the OH-related bond, S_{OH2}, on the water vapor annealing time t_w after the dry case. "0" and "60 min" on the horizontal axis mean the 60-min dry NH_3 annealing without water vapor and the 60-min water-added NH_3 annealing, respectively. Also, "45 min" means a process in which the first gas is dry NH_3 for 15 min and the subsequent gas is water-added NH_3 for 45 min, as shown in the inset. From this figure, it can be seen that t_w needs more than 30 min to reduce S_{OH2} more than that of the 60 min dry case, i.e. $t_w = 0$. However, in the opposite case, where the first gas is water-ad.ded NH_3 for 30 min and the subsequent gas is dry NH_3 for 30 min, S_{OH2} is much smaller than previously at $t_w = 30$ min and the same level as that of the 60-min water-added case. This seems strange because the annealing times for the first and the second gases are the same, 30 min. Next, we used a shorter total annealing time of 30 min for both the dry and water-added cases. Figure 4 shows the S_{OH2} values at total annealing times t_a of 30 and 60 min for the dry (blue closed circles) and water-added (green closed triangles) NH_3 gases, in addition to the data of the 30 min dry → 30 min water (blue open circle), the reverse (green open triangle) in Fig. 3, and only N_2 (no NH_3) gas (black closed circles) processes for comparison. In this figure, $t_a = 0$ is in an equivalent state to an as-deposited film. It can be observed from Fig. 4 that S_{OH2} in the $NH_3 + N_2$ cases is much lower than that in the only N_2 gas case due to the lack of the catalytic effect of NH_3 in the latter case. Further, it can be seen that the reduction rate of S_{OH2} with t_a for the added water vapor case is clearly higher than that of the dry case within 60 min, which is coincident with the result of Fig. 2. However, the blue and green open marks at $t_a = 60$ min, in which the process gases were changed at 30 min, are the almost same as the blue and green closed ones, respectively. This means that the concentration of OH bonds is almost governed by the annealing atmosphere used for the initial 30 min, regardless of the annealing gas for the subsequent 30 min. The blue broken and green dotted broken lines are the fitting curves based on a simple theoretical model for the annealing time dependence of S_{OH2}, which is mentioned and discussed in detail later in Sect. 4, as well as the experimental data in Fig. 4.

Figure 5 shows the FT-IR spectra around the TO_3 mode peak of the Si-O-Si bond from 800 to 1300 cm^{-1} of the annealed samples with water vapor times t_w of 0, 30, and 60 min shown in Fig. 3 for the process of dry → water-added NH_3 gas. In addition, the spectrum of the as-deposited film is shown as a standard. It can be observed from Fig. 5 that the peak positions are shifted with the increasing t_w, and that the shift amount is almost saturated within $t_w = 30$ min. Figure 6 shows the dependences of the wavenumber range in the TO_3 mode peak on the annealing process, including the case of the as-deposited film as a reference. The processes are dry, water-added, dry → water-added, and water-added → dry. The annealing times for the entire dry and water-added processes are 30 and 60 min. The wavenumbers $k_p'_{min}$, k_p, and $k_p'_{max}$ shown in this figure are the positions of the first derivative minimum, the peak, and the first derivative maximum, respectively. Also, as a reference, those of a 100 nm thermal

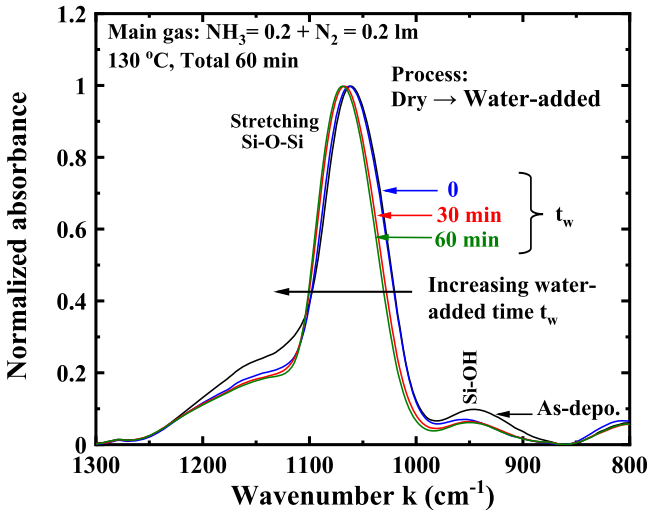

Fig. 5. FT-IR spectra around the TO_3 mode peak of Si-O-Si bond from 800 to 1300 cm^{-1} of the annealed samples with $t_w = 0$ (blue line), 30 (red line), and 60 min (green line) as shown in Fig. 3 for the dry → water-added NH_3 gas process. As a standard, the as-deposited one (black line) is shown.

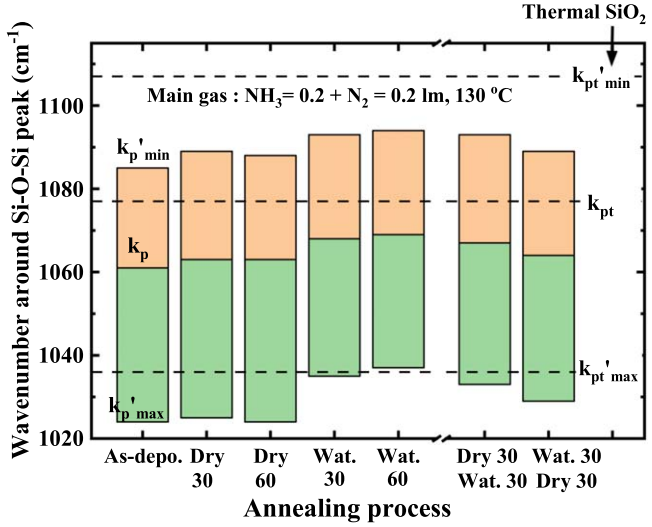

Fig. 6. Histogram of the annealing process and the extension range in wavenumbers k of the TO_3 mode peak of the annealed SiOx films. The characteristics of $k_p'_{min}$, k_p, and $k_p'_{max}$ are wavenumber positions at the first derivative minimum, the peak, and the first derivative maximum, respectively, of the mode. As references, those of 100 nm thick thermal SiO_2 are shown as broken lines with labels of $k_{pt}'_{min}$, k_{pt}, and $k_{pt}'_{max}$. The abbreviation "Wat." indicates the water-added NH_3 gas process, and the figures after the respective processes indicate the annealing times. For example, "Dry 30 Wat. 30" means the dry NH_3 gas process for 30 min followed by the water-added NH_3 gas process for 30 min.

SiO_2 film formed at 1000 °C are indicated by the broken lines as labels of $k_{pt}'_{min}$, k_{pt}, and $k_{pt}'_{max}$. The region areas from $k_p'_{min}$ to k_p and k_p to $k_p'_{max}$ are colored in light-orange and light-green, respectively, and then the k_p positions are just at the boundaries of each region. Since the TO_3 mode peak is unsymmetric, the $k_p'_{min}$ and $k_p'_{max}$ positions are unsymmetric with respect to k_p. Table I shows the wavenumbers (cm^{-1}) at $k_p'_{min}$, k_p, and $k_p'_{max}$ for the respective annealing processes. As a reference, the data of the as-deposited film (process time = 0) are shown. It is well known that a peak position k_p of the TO_3 mode can be approximated by an expression of the form

$$k_p = \frac{\alpha}{m_O}(1 - \cos\theta) + \frac{4}{3}\frac{\alpha}{m_{Si}}, \quad (2)$$

where α is the Si-O stretching force constant, m_O and m_{Si} are the masses of the oxygen and the silicon atoms, respectively, and θ is an Si-O-Si inter tetrahedral bond angle.[17,20,29] The width of the peak can also be understood in terms of the statistical distribution of θ and summation over narrow angles. Therefore, the change in k_p, $k_p'_{min}$, and $k_p'_{max}$ as shown in Fig. 6 can be regarded as a change in the SiOx film structure.[19] In addition, as can be found easily from Fig. 6, the characteristics related with k_p for the low-temperature-deposited SiOx films are almost lower than those of the thermal SiO_2 film, with the exception of $k_p'_{max}$ in the water-added case. According to Eq. (2), lower values of the k_p characteristics suggest that the angle θ and/or α should be lower than those of thermal SiO_2 film. This tendency coincides with that observed in many previous reports.[10,15,17,30] It can be explained by the fact that lower-temperature-deposited SiOx films contain more OH bonds. When the OH bonds are removed due to dehydroxylation during deposition or cooling down from the deposition temperature, the SiOx films are shrunk and densified more or less[10,11,31,32] so that the films are compressively stressed. This stress leads to a lower θ or k_p. Further, when the stressed films are annealed, further reduction of the OH bond occurs, and the films are more stressed or relaxed, which is dependent on annealing conditions. Then, the structures of the annealed SiOx films may be changed from those of the untreated ones so that we can observe different forms of the peak, depending on the annealing conditions, such as the temperature. Generally, it is reported that k_p is shifted upward after thermal treatment such as annealing because the structure of the strained SiOx films becomes less stress and relaxed due to the treatment, approaching a state like thermal SiO_2 film. Further, we can see from Fig. 6 that the structural change of the low-temperature SiOx films by annealing with the water-added NH_3 gas is very different from that observed with the dry one. So, it can be inferred that the change in the SiOx film structure is related to the dynamics in the chemical reduction of OH bonds in the film, in light of the results shown in Figs. 2, 3, and 4. These results are discussed deeply in relation to the mechanism of OH bond removal due to the water vapor in the next section.

4. Discussion

Before the discussion, we checked whether the water vapor itself has dehydroxylation action on the Si-OH bond or not. Figure 7 shows the FT-IR spectra of the SiOx films annealed by only N_2 gas with and without water vapor, compared with that of the as-deposited film. We notice surprisingly from Fig. 7 that, even without NH_3 gas, the intensities of not only the OH2 but also the OH1 peak are decreased more by adding water vapor into the N_2 gas. This result means that water vapor itself has an effect of enhancement on the removal of OH bonds. Similar results have been reported using high water vapor pressure $>1 \times 10^5$ Pa and temperature >200 °C.[33,34]

According to Eq. (1), we can assume that rate of the dehydroxylation reaction is proportional to the square of the OH concentration or S_{OH2} value. Therefore, the reaction rate

Table I. Wavenumbers (cm^{-1}) at the first derivative minimum $k_{p'min}$, the peak k_p, and the first derivative maximum $k_{p'max}$ of the TO_3 mode peak for the respective annealing processes. As a reference, the data of the as-deposited film (process time = 0) are shown.

Process time (min)	As-deposited 0	Dry 30	Dry 60	Water 30	Water 60	Dry→Water 30 →30	Water→Dry 30 →30
$k_{p'min}$ (cm^{-1})	1085	1089	1088	1093	1094	1093	1089
k_p (cm^{-1})	1061	1063	1063	1068	1069	1067	1064
$k_{p'max}$(cm^{-1})	1024	1025	1024	1035	1037	1033	1029

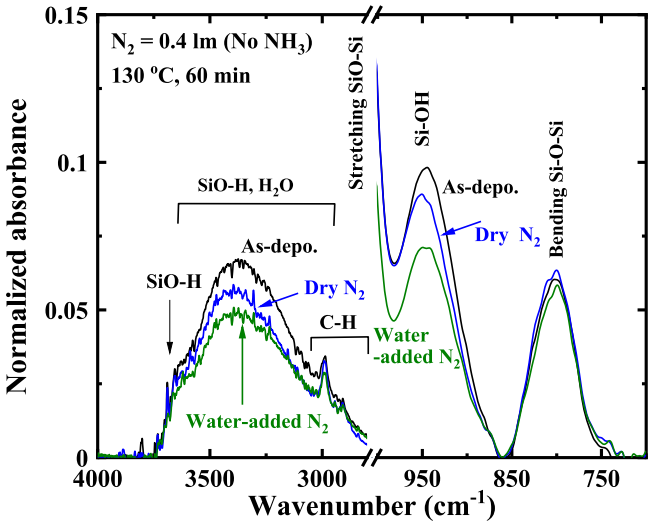

Fig. 7. FT-IR spectra of the SiOx films annealed by only N_2 gas (no NH_3) with and without water vapor, compared with that of the as-deposited film.

equation of dehydroxylation between two Si-OH bonds can be written simply as

$$\frac{dS_{OH2}}{dt_a} = -AS_{OH2}{}^2, \tag{3}$$

and its solution is solved easily as

$$S_{OH2} = \frac{S_{OH20}}{A{\cdot}S_{OH20}{\cdot}t_a + 1}, \tag{4}$$

where $A > 0$ is a rate constant ($1/(cm^{-1}{\cdot}min)$) and S_{OH20} (cm^{-1}) is an initial condition of S_{OH2} at $t_a = 0$. In Fig. 4, the calculated fitting curves for the dry (blue broken line) and the water-added (green dotted broken line) cases are drawn using a least-squares method. The fitting parameters of A for the dry and the water-added cases are calculated as $A_D = 0.00044$ and $A_W = 0.00076$ ($1/(cm^{-1}{\cdot}min)$), respectively. This means that the dehydroxylation rate of the water-added NH_3 case is higher than that of the dry one. It can also be seen that both fitting curves show a relatively good agreement with the data within 60 min, although the fitting degrees are not excellent. So, we can say that the fitting curves reveal essential phenomena in physics in this experiment. The not-so-good fitting is probably due to the non-ideal reaction, which is different from Eq. (1), e.g. the influence of residual H_2O molecules, other complicated structural defects in the films, and so on. A small number of data and lack of data for long annealing time are other factors. So, further study of the dehydroxylation rate is required in the future.

D'Souza et al. have reported hydroxylation and dehydroxylation of silica glass as follows:[35] When a defective, e.g. scribed surface of amorphous silica is exposed to the ambient environment, it will minimize such a high-energy surface state by adsorbing water from the atmosphere. That is, the surface layer gets hydroxylated and many Si-OH bonds are formed on it. On dehydroxylation again from the hydroxylated surface, the condensation of these silanol groups reforms various kinds of strained Si-O-Si bonds, among which some bonds are probably highly strained. Since the highly strained Si-O-Si bonds are assumed to have high strain energy, they should be more easily hydroxylated again or rehydroxylated. Conversely, if Si-O-Si bonds formed by dehydroxylation are less strained, they will not be easily rehydroxylated. Also, in terms of the glass structure, it has been reported that Si-O-Si bonds with a smaller θ than in the thermal equilibrium case have strained Si-O bonds, which are highly reactive due to the high energy state, compared to unstrained bonds.[36–38] Actually, it has been reported that the etch rate of glass is increased with the decreasing θ, and that when the average Si-O-Si bond angle θ decreases, the water solubility is increased due to the promotion of the reaction between silica glass and molecular water to form hydroxyl groups attached to the silica network as silanol (Si-OH).[39] Furthermore, Michalske et al. have given the following suggestions from their experimental and molecular-orbital calculation results:[36] (1) Extension of the Si-O-Si angles toward 180° induces only small stress-energy changes and has little effect on the chemistry of the Si-O-Si bond. (2) Si-O bond length extension requires a large amount of energy, but has only a moderate impact on reactivity, which is not expected to be important in the formation of an active site. (3) When θ becomes lower, which is opposite to (1), the change in angle increases the reactivity of the strained bond. From these reports, it can be expected that chemical reaction sites to form silanol groups are strained bonds with smaller θ less than the standard or stress-free value, e.g. that of the thermal SiO_2 film.

Considering the above reports and the results of Figs. 4, 6, and 7, we discuss the effect of water vapor on the reduction of OH bonds. Figure 8 shows schematic models of the Si-O-Si bond network for (a) the as-deposited film, (b) the dry, and (c) the water-added cases. In (a), provisionally, all of the top Si atoms are terminated with hydroxyls -OHs. On the other hand, in (b) and (c), due to the dehydroxylation reaction, -OH bonds are removed and Si-O-Si bridge bonds are formed, but their distributions of the bond angle value θ are different from each other as shown in Fig. 6. That is, in (b), for the dry case with lower k_p, the number of bonds with low angles θ_L is larger than that with high angle θ_H, and vice versa in (c) for the water-added case with higher k_p. Next, we consider the reason why the water-added case has a larger amount of bonds with θ_H than the dry case. When H_2O molecules approach a Si-O-Si bond network like in Fig. 9(a), which is the same as Fig. 8(b), H_2O react with the highly strained or high energy bonds with θ_L. Then, the six Si-O bonds are

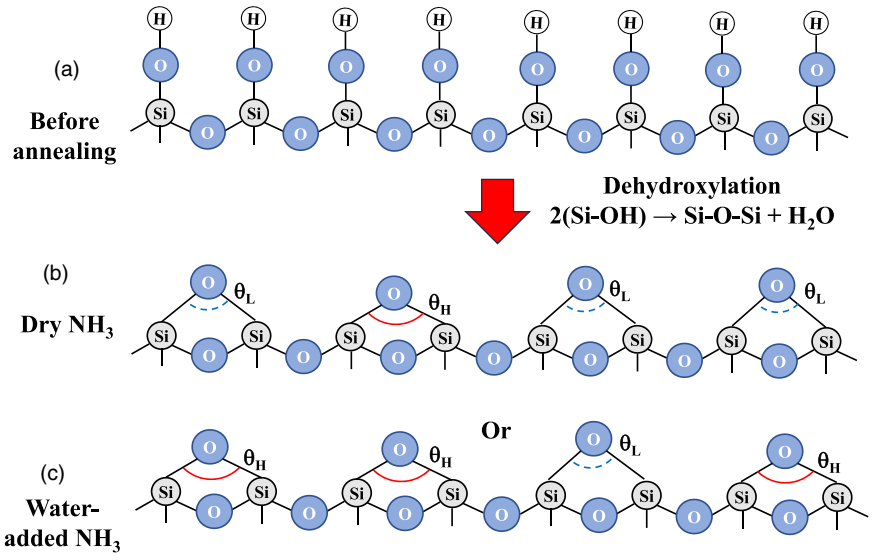

Fig. 8. Schematic models of Si-O-Si network to explain the experimental results. (a) is as-deposited SiOx film, (b) and (c) are SiOx films annealed by the dry and the water-added NH_3 gas, respectively. In (a), all of the top Si atoms are terminated with hydroxyls -OHs, and Si-OH are formed. θ_L and θ_H shown in (b) and (c) are low and high bridge angles of Si-O-Si bonds, respectively. An Si-O-Si bond with low θ_L is more unstable or in a higher energy state than that with high angle θ_H since the bond with θ_L is highly strained compared with that with θ_H. The actual reaction occurs not only on the surface but also in the film bulk.

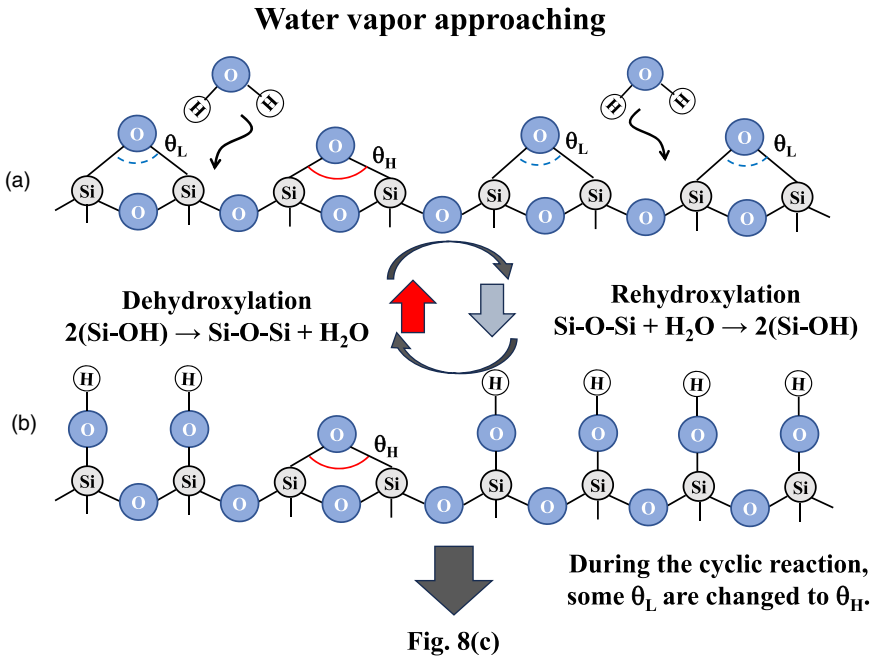

Fig. 9. Schematic models of Si-O-Si bridge bond networks (a) before and (b) after hydroxylation due to reaction with water vapor in the annealing atmosphere. The (a) model has three low θ_L and one high θ_H in the top Si-O-Si bonds. The (b) model has six hydroxylated bonds, which are generated from the three bonds with θ_L in the high strain energy state in Fig. 9(a). (a) and (b) reactions are repeated continuously until annealing process is finished. If the annealing time in the water-added case is 60 min, the resultant configuration of the Si-O-Si network may become like the one shown in Fig. 8(c). Actually, since these reactions occur three-dimensionally in space as well as two-dimensionally, recombination due to dehydroxylation develops not only between the previously bonded atoms but also other neighbors.

broken up and the six Si atoms are terminated with an -OH bond subsequently. As a result, the six Si-OH groups are produced as shown in Fig. 9(b). However, they are dehydroxylated again immediately due to the catalytic effect of NH_3 gas in the annealing atmosphere in spite of the existence of water vapor. Here, we should note the formation of the new bond angle θ. Since the large amount of OH bonds is much reduced from the as-deposited film as shown in Fig. 2(b), the water vapor should not only reach the surface but also diffuse in the film bulk as well as NH_3 gas. This is because the result of Fig. 2 is difficult to explain reasonably without the diffusion in the film bulk of water vapor and NH_3 gas. In addition, the actual reaction space is not two but three dimensions, although Figs. 8 and 9 show the vicinity of the surface area two-dimensionally in a simple way for easy understanding. Since Si-OH bonds are actually in a three-dimensional Si-O-Si network or in film bulk, they have a chance to recombine with not only the previously combined one but also other neighbors. Therefore, a newly formed θ does not always have the same value as before. After the dehydroxylation, if a bond angle θ of the new Si-O-Si bond is low $\lesssim \theta_L$, the new strained bond with high energy is probably

rehydroxylated again due to the water vapor as in Fig. 9(b), and then dehydroxylation occurs between -OHs again with a small change of the atomic structural configuration of the Si-O-Si network. If the new θ is high $\gtrsim \theta_H$, the dehydroxylated Si-O-Si bond is likely to roughly keep the state of θ_H, and is not broken due to its high stability. The cyclic reaction routine between dehydroxylation and rehydroxylation shown in Figs. 9(a) and 9(b) probably continues until an unstable Si-O-Si bond changes to a stable one with high $\theta \gtrsim \theta_H$. When the annealing time is 60 min or not sufficient for reaction, the resultant configuration of the Si-O-Si network may turn into one like that shown in Fig. 8(c).

Finally, we discuss the contrasting results of the annealing processes of "Dry 30 min → Water-added 30 min" (Process D-W) and "Water-added 30 min → Dry 30 min" (Process W-D), which are shown in Figs. 3 and 4, taking (Eq.3) into account. The former and latter results present almost the same S_{OH2} values as "Dry 60 min" and "Water-added 60 min", respectively, although D-W and W-D have different sequential processes with a half annealing time of 30 min. In the D-W process, the initial dry 30 min process forms new Si-O-Si bonds due to dehydroxylation from -OH bonds of the as-deposited film, where some of the Si-O-Si bond angles including the new ones spread into the lower θ_L region. However, just after 30 min or changing the process from "Dry" to "Water-added", most of the Si-O-Si bonds in the lower θ_L region are probably rehydroxylated due to water vapor immediately, so that a lot of new -OH bonds are generated abruptly. Then, due to the dehydroxylation effect of NH_3, the OH bonds including the remaining ones are gradually reduced with a low A in (Eq. 2) similar to the dry process A_D even in the water-added process due to the abrupt abundant generation of OH bonds. On the other hand, for the opposite case of the W-D process, by the initial "Water-added" process for 30 min, most of the Si-O-Si bonds in the lower θ_L region of the as-deposited film transition to the higher θ_H region and become relatively more stabilized. So, even in the latter process of the dry NH_3 atmosphere, it may take some time, i.e. more than 30 min, for the transitioned bonds to return to a state in the lower θ_L region perfectly, probably due to their higher stable state with θ_H. So, even after the dry 30 min process, A stays roughly similar to A_W of the water-added 60 min (green closed triangle) so that the 60 min S_{OH2} value (green open triangle) is the almost same as that of the water-added 60 min. If the annealing time for the latter water-added and dry processes in the D-W and W-D processes, respectively, are elongated much longer than 30 min, their final resultant S_{OH2} values would asymptotically approach those obtained by the water-added and dry processes, respectively, throughout the long annealing time. However, in order to explain this quantitatively, further investigation is needed.

5. Conclusions

We investigated an effective method to remove OH bonds in low-temperature-deposited SiOx films by annealing with NH_3 gas at 130 °C in atmospheric pressure. We found that adding water vapor into NH_3 gas is more effective at reducing OH bonds than only dry NH_3 gas. Also, the FT-IR spectra showed a difference in the structure of the annealed SiOx films between the water-added and the dry NH_3 cases, in which the peak of the Si-O-Si bond was shifted toward a higher wavenumber in the water-added case. We considered the mechanism of the water vapor effect on the reduction of OH bonds to be as follows: after flowing the water-added NH_3 gas into the reactor, Si-OH bonds are immediately dehydroxylated due to the NH_3 catalytic effect, which leads to the formation of strained Si-O-Si bridge bonds due to the film contraction caused by the dehydroxylation. The strained bonds cause the bond angle θ of Si-O-Si to be smaller θ_L than that of the stress-free bond. Then, highly strained Si-O-Si bonds are rehydroxylated easily to form Si-OH + Si-OH bonds again in the water vapor atmosphere since they are in a higher energy state, or more unstable. However, owing to the catalytic effect of NH_3 gas in the annealing atmosphere, the silanol bonds are dehydroxylated again. Therefore, rehydroxylation and dehydroxylation are repeated continuously until the Si-O-Si bond formed by dehydroxylation is less strained with $\theta \geqslant \theta_H$, where θ_H is the higher angle of the Si-O-Si bond in the less strained energy state. As a result, the amount of residual OH bonds is less than that in the dry NH_3 annealing case. Also, the portion of less strained bonds with θ_H in the water-added NH_3 case is obviously larger in SiOx films than in the dry case. This is the difference in structure of the annealed SiOx films between the water-added and the dry annealing cases.

Acknowledgments

This research was partially supported by JSPS KAKENHI, Grant No. JP21K04649.

1) S. Higashi, D. Abe, S. Inoue, and T. Shimoda, Jpn. J. Appl. Phys. **40**, 4171 (2001).
2) M. M. Moslehi, R. A. Chapman, M. Wong, A. Paranjpe, H. N. Najm, J. Kuehne, R. L. Yeakley, and C. J. Davis, IEEE Trans. Electron Devices **39**, 4 (1992).
3) T. Kawahara, A. Yuuki, and Y. Matsui, Jpn. J. Appl. Phys. **31**, 2925 (1992).
4) K. Murase, N. Yabumoto, and Y. Komine, J. Electrochem. Soc. **140**, 1722 (1993).
5) M. Yoshimaru and T. Yoshie, J. Electrochem. Soc. **145**, 2847 (1998).
6) J. Arnó, Z. Yuan, and S. Murphy, J. Electrochem. Soc. **146**, 276 (1999).
7) Y. Nishi, T. Funai, H. Izawa, T. Fujimoto, H. Morimoto, and M. Ishii, Jpn. J. Appl. Phys. **31**, 4570 (1992).
8) M. Matsuura, Y. Hayashide, H. Kotani, and H. Abe, Jpn. J. Appl. Phys. **30**, 1530 (1991).
9) T. Ito, T. Matumoto, and K. Nishioka, Surf. Coatings Technol. **215**, 447 (2013).
10) S. Horita, K. Toriyabe, and K. Nishioka, Jpn. J. Appl. Phys. **48**, 035502 (2009).
11) S. Horita, Jpn. J. Appl. Phys. **58**, 038002 (2019).
12) S. Horita, Proc. 31th Int. Workshop Active-Matrix Flatpanel Displays and Devices (AM-FPD"24), 2024, p. 199.
13) S. Horita and P. Jain, Jpn. J. Appl. Phys. **56**, 088003 (2017).
14) S. Horita and P. Jain, Jpn. J. Appl. Phys. **57**, 03DA02 (2018).
15) P. Lange, U. Schnakenberg, S. Ullerich, and H-J. Schliwinski, J. Appl. Phys. **68**, 3532 (1990).
16) A. Barranco, F. Yubero, J. Cotrino, J. P. Espinós, J. Benítez, T. C. Rojas, J. Allain, T. Girardeau, J. P. Rivière, and A. R. González-Elipe, Thin Solid Films **396**, 9 (2001).
17) P. Innocenzi, P. Falcaro, D. Grosso, and F. Babonneau, J. Phys. Chem. B **107**, 4711 (2003).
18) A. Savizky and M. J. E. Golay, Anal. Chem. **36**, 1627 (1964).
19) S. Horita and D. Pu, Jpn. J. Appl. Phys. **63**, 01SP12 (2024).
20) R. M. Almeida and C. G. Pantano, J. Appl. Phys. **68**, 4225 (1990).
21) F. L. Galeener, Phys. Rev. B **19**, 4292 (1979).
22) P. G. Pai, S. S. Chao, Y. Takagi, and G. Lucovsky, J. Vac. Sci. Technol. A **4**, 689 (1986).

23) G. Lucovsky, M. J. Manitini, J. K. Srivastava, and E. A. Irene, J. Vac. Sci. Technol. B **5**, 530 (1987).
24) J. T. Fitch, G. Lucovsky, E. Kobeda, and E. A. Irene, J. Vac. Sci. Technol. B **7**, 153 (1989).
25) N. Hirashita, S. Tokitoh, and H. Uchida, Jpn. J. Appl. Phys. **32**, 1787 (1993).
26) M. A. Natal-Sanyiago and J. A. Dumesic, J. Catal. **175**, 252 (1998).
27) T. Luts and A. Katz, Top. Catal. **55**, 84 (2012).
28) T. Luo, R. Zhang, W-W. Zeng, C. Zhou, X. Yang, and Z. Ren, J. Phys. Chem. C **125**, 8638 (2021).
29) A. Fidalgo and L. M. Ilharco, J. Non-Cryst. Solids **283**, 144 (2001).
30) P. Lange, J. Appl. Phys. **66**, 201 (1989).
31) C. Cobianu, C. Pavelescu, and V. M. Catuneanu, J. Matter. Sci. Lett. **6**, 23 (1987).
32) H. Kato, H. Sakai, and K. Sugawara, J. Electrochem. Soc. **141**, 3154 (1994).
33) T. Sameshima and M. Satoh, Jpn. J. Appl. Phys. **36**, L687 (1997).
34) T. Sameshima, K. Sakamoto, Y. Tsunoda, and T. Saitoh, Jpn. J. Appl. Phys. **37**, L1452 (1998).
35) A. S. D'Souza and C. G. Pantano, J. Am. Ceram. Soc. **85**, 1499 (2002).
36) T. A. Michalske and B. C. Bunker, J. Appl. Phys. **56**, 2686 (1984).
37) B. C. Bunker, D. M. Haaland, T. A. Michalske, and W. L. Smith, Surf. Sci. **222**, 95 (1989).
38) T. A. Michalske and B. C. Bunker, J. Am. Ceram. Soc. **76**, 2613 (1993).
39) A. Agarwal and M. Tomozawa, J. Non-Cryst. Solids **209**, 166 (1997).